Single photon emission at 1.55m from charged and neutral exciton confined in a single quantum dash

. Dusanowski, M. Syperek, P. Mrowiski, W. Rudno-Rudziski, J. Misiewicz, A. Somers, S. Höfling, M. Kamp, J. P. Reithmaier, and G. Sk

Articles you may be interested in

Photoluminescence studies on self-organized 1.55-m InAs/InGaAsP/InP quantum dots under hydrostatic pressure
J. Appl. Phys. **116**, 023510 (2014); 10.1063/1.4890013

Exciton and biexciton dynamics in single self-assembled InAs/InGaAlAs/InP quantum dash emitting near 1.55m
Appl. Phys. Lett. **103**, 253113 (2013); 10.1063/1.4852736

Telecom-wavelength (1.5m) single-photon emission from InP-based quantum dots
Appl. Phys. Lett. **103**, 162101 (2013); 10.1063/1.4825106

Carrier relaxation dynamics in InAs/GaInAsP/InP(001) quantum dashes emitting near 1.55m
Appl. Phys. Lett. **103**, 083104 (2013); 10.1063/1.4818759

Impact of the capping layers on lateral confinement in InAs InP quantum dots for 1.55 m laser applications studied by magnetophotoluminescence
Appl. Phys. Lett. **87**, 233111 (2005); 10.1063/1.2132527

Single photon emission at 1.55 μm from charged and neutral exciton confined in a single quantum dash

Ł. Dusanowski,[1,a)] M. Syperek,[1] P. Mrowiński,[1] W. Rudno-Rudziński,[1] J. Misiewicz,[1] A. Somers,[2] S. Höfling,[2,3] M. Kamp,[2] J. P. Reithmaier,[2,4] and G. Sęk[1]

[1]Institute of Physics, Wrocław University of Technology, Wybrzeże Wyspiańskiego 27, 50-370 Wrocław, Poland
[2]Technische Physik, University of Würzburg, Wilhelm-Conrad-Röntgen-Research Center for Complex Material Systems, Am Hubland, D-97074 Würzburg, Germany
[3]School of Physics and Astronomy, University of St. Andrews, North Haugh, KY16 9SS St. Andrews, United Kingdom
[4]Institute of Nanostructure Technologies and Analytics (INA), CINSaT, University of Kassel, Heinrich-Plett-Str. 40, 34132 Kassel, Germany

We investigate charged and neutral exciton complexes confined in a single self-assembled InAs/InGaAlAs/InP quantum dash emitting at 1.55 μm. The emission characteristics have been probed by measuring high-spatial-resolution polarization-resolved photoluminescence and cross-correlations of photon emission statistics at T = 5 K. The photon auto-correlation histogram of the emission from both the neutral and charged exciton indicates a clear antibunching dip with as-measured $g^{(2)}(0)$ values of 0.18 and 0.31, respectively. It proves that these exciton complexes confined in single quantum dashes of InP-based material system can act as true single photon emitters being compatible with standard long-distance fiber communication technology. © 2014 AIP Publishing LLC.
[http://dx.doi.org/10.1063/1.4890603]

Single self-assembled quantum dots (QDs) and other quantum dot-like nanostructures emitting near the 1.3 μm and 1.55 μm[1–4] have attracted much attention lately. This interest originates in the important role that true single photon sources (SPS) play in quantum communication,[5] i.e., they enable one to establish low-loss quantum links in the optical fiber-based short and long-haul communication. The attractiveness of a self-assembled QD with respect to other quantum emitters is mainly related to its relatively easy integration with today's semiconductor-based optoelectronic technologies. Incorporation of a QD into a high quality microcavity[6] can result in a bright and optically or electrically driven single photon source[7,8] with impressive photon extraction efficiency,[9,10] photon indistinguishability,[11] variable photon generation rate, and coherent control of the emission process.[12,13] Despite that, experimental attempts to obtain such systems in the telecommunication spectral range are very rare,[1–4] especially, near the 1.55 μm photon wavelength, which defines the telecom C-band.[2–4] Single quantum dot emission in that range has been demonstrated for a few kinds of nanostructures: colloidal PbS nanocrystals,[14] InN nanopyramids,[15] metamorphic InAs/(In,Ga)As QDs,[16] InAs/InP QDs,[2–4] and InAs/GaAs QDs utilizing frequency down-conversion scheme.[17] Among the listed solutions, single photon emission has only been demonstrated for the last two. Nevertheless, further efforts are still necessary to find the most suitable SPS operating at 1.55 μm photon wavelength. We show that the InAs/InP quantum dash (QDash) can also be considered as a key element of an SPS.

Most of the implemented SPSs are based on the QD ground state neutral exciton (X) emission, which exhibits fine structure, engineering of which is a framework for creating entangled photons by a biexciton-exciton cascade recombination.[18] Such a quantum system is desired for some of the quantum cryptography applications.[7] On the other hand, the lack of the fine structure splitting of the charged exciton (CX) results in higher single-photon emission repetition rates compared to the neutral exciton ones.[9] Up to date, almost no reports exist concerning single QD emission from the charged exciton state at the telecommunication wavelengths, except for an example at 1.3 μm,[19] and despite its additional importance for long-lived spin quantum memories.[20] In this Letter, we report the demonstration of single photon emission from an InAs/InGaAlAs/InP QDash by both charged and neutral exciton complexes recombining radiatively near 1.55 μm.

The investigated sample was grown in an EIKO gas source molecular-beam epitaxy system on an S-doped InP(001) substrate. The layered sequence starts from a 200 nm-thick $In_{0.53}Ga_{0.23}Al_{0.24}As$ layer lattice matched to InP, which was grown on the substrate at 500 °C. In order to form QDashes in a self-assembled way, an InAs layer with a nominal thickness of 1.3 nm was deposited at 470 °C, out of which quantum dash structures on a wetting layer were formed. The QDashes were covered by a 100 nm-thick $In_{0.53}Ga_{0.23}Al_{0.24}As$ layer and subsequently capped with a 10 nm-thick layer of InP. The lateral dimensions of QDashes are about 20 nm in width and between 50 and hundreds of nanometers in length, whereas their height is 3.5 nm.[21] Since the planar density of QDashes is rather high, 10^{11} cm^{-2}, a combination of electron beam lithography and reactive ion etching techniques has been used to produce mesa structures with different sizes

a)Author to whom correspondence should be addressed. Electronic mail: lukasz.dusanowski@pwr.edu.pl.

down to $0.2\,\mu m^2$ ($600 \times 300\,nm^2$) in order to resolve emission from single dashes of an inhomogeneous ensemble.

For all the experiments, the sample was kept in a liquid-helium continues-flow cryostat at T = 5 K. Spatially resolved photoluminescence spectroscopy and photon cross-correlation statistic measurements have been performed using a micro-photoluminescence (μPL) setup providing a spatial resolution on the order of a single μm, and a spectral resolution of approximately 100 μeV. The sample was excited with a 787 nm line of a continuous-wave semiconductor diode laser. The emission intensity of the isolated spectral lines has been detected by a liquid nitrogen-cooled InGaAs-based linear array detector combined with a 0.3 m focal length single grating monochromator. The modified setup with a 1 m-long monochromator has been used to determine the polarization properties of the selected individual emission lines. This setup allows obtaining the spectral resolution of approximately 30 μeV. The degree of linear polarization has been measured by rotating a half-wave plate inserted in front of a linear polarizer placed at the monochromator entrance slit. Photon cross-correlation experiment was conducted with a Hanbury Brown and Twiss interferometer.[22] In this case, two short focal length monochromators were used as spectral filters for the selected wavelengths corresponding to the X and CX emission. Each of the monochromator outputs was equipped with a fiber-coupled NbN superconducting single-photon detector with 15% quantum efficiency and 10 dark counts/s at 1.55 μm. The photon correlation statistics was acquired by a multichannel picosecond event timer. Distinction between the charged and neutral excitons has mainly been made based on linear-polarization-resolved measurements and the lack of fine structure splitting for the CX in contrast to the X emission line,[23,24] additionally supported by cross-correlation of the photon emission from both X and CX complexes exhibiting a characteristic line shape of the second order correlation function.[24,25]

Figure 1(a) presents a low-temperature (T = 5 K) μPL spectrum consisting of a neutral (at 0.7988 eV) and charged exciton (at 0.7948 eV) emission features from a single InAs/InGaAlAs/InP QDash. The energy distance between both spectral lines is about 4 meV, which defines the charged exciton binding energy in this QDash. The intensities of both lines do not deviate significantly from the linear dependence with excitation power in the low excitation regime (not presented here). Details about other excitonic complexes, like biexcitons and the biexciton-exciton cascade emission process in such InAs/InGaAlAs/InP QDashes have been reported previously.[26]

Under the most typical excitation scheme, a QD/QDash is driven non-resonantly by the laser pulse (our case) or electrical carrier injection. Accordingly, electrons and holes are created in the high energy continuum of states and subsequently follow the energy relaxation towards the QD/QDash ground state, where an exact excitonic complex is finally settled. Due to the neutral exciton fine structure governed by the lack of full rotational symmetry in the QDash plane, the X state is built from the states described by the total angular momentum projection of $J_z = \pm 1$ or $J_z = \pm 2$, as presented in Fig. 1(c). In the former case, the exciton couples to the photon field ("bright" states) in contrast to the latter, where the
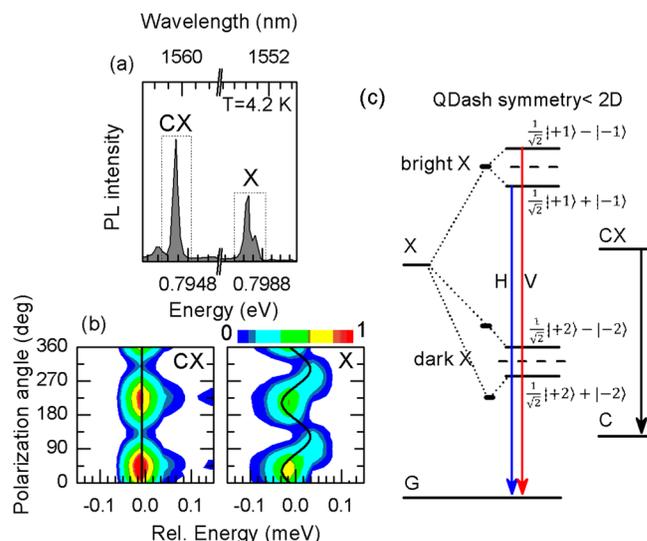

FIG. 1. (a) Low temperature microphotoluminescence spectra for X and CX confined in InAs/InP quantum dash; pump power density, 6 W/cm^2 (measured outside the cryostat). (b) Polarization resolved microphotoluminescence spectra map for X and CX. Exciton fine structure splitting is on the level of 60 μeV. (c) Single quantum dash recombination scheme including exciton fine structure.

X emission is dipole forbidden ("dark" states). Therefore, in the case of a random carrier capture, a neutral exciton can be loaded into a QDash either in a "bright" or a "dark" state. The "bright" exciton can additionally be formed directly from a biexciton recombination process, or by spin-flip acts from a "dark" exciton state. This leads to existence of some uncertainty in the on demand generation of a "bright" exciton, and therefore, it results in a restriction of the maximal achievable QD/QDash emission rate.[13] In order to avoid the "dark" state impact on a single photon generation process, a QDash can be directly loaded with a charged exciton. An additional residual carrier in the QD/QDash confining potential can be supplied either through electrical gates[9,27] or intentional doping of a dot/dash.[15,20,28] Existence of residual dopants or defect states can also lead to the presence of an additional charge in the nano-object. Since the CX state represents a spin singlet state, the exchange interaction is effectively cancelled. Consequently, the CX has no fine structure (see Fig. 1(c)). In such a case, recombination is always expected to be "bright" and CX-based SPS can continuously generate single photons with rates approaching the inverse of the CX lifetime. The CX-based SPS has already been demonstrated in the GaAs material system, where an increase in the photon emission efficiency by a factor of three has been obtained when compared to neutral exciton based SPS.[9]

Polarization resolved-μPL experiment can give important insight into the nature of the observed emission states. Figure 1(b) shows spectral evolution of the X and CX emission lines as a function of the linear polarizer angle. The X emission exhibits clearly the oscillatory-like character of the linear polarization, which is governed by the existence of the fine structure splitting (approximately 60 μeV, in this case). What is more important, the CX emission shows no polarization dependence, which confirms the lack of the fine structure as expected for the charged exciton state. These experimental results do not evidence whether the discussed

CX and X states are formed in the same QDash. Therefore, the measurement of the second order cross-correlation function has been performed for the X-CX emission, which acts in the continuous-wave excitation mode, see Figure 2. The photon cross-correlation histogram indicates a slightly asymmetric antibunching dip with the as-measured $g^{(2)}(0) = 0.3$. The experimental trace can be accurately fitted (see red solid line in Fig. 2) using a five level rate equation model detailed in Ref. 29, while the characteristic lifetimes are taken from our previous experiments.[26] These findings unambiguously indicate that both lines originate from the same confined space, and confirm the charged exciton character of the line assigned previously as CX. We expect CX to be rather a negatively charged complex since InP shows typically n-doping background in the order of 10^{15} cm^{-3}. Such interpretation is also consistent with binding energy calculations performed for symmetric InAs/InP QDs.[30]

The photon number distribution for the CX and X state can be directly probed by measuring the second order auto-correlation function $g^{(2)}$. Figures 3(a) and 3(b) show low temperature ($T = 5$ K) auto-correlation histograms for neutral and charged exciton emission processes, respectively. Both the $g^{(2)}$ functions show a clear photon antibunching dip at the zero time delay ($\tau = 0$). The as-measured $g^{(2)}_{CX-CX}(\tau = 0)$ value for the CX state reaches 0.31, whereas for the neutral exciton $g^{(2)}_{X-X}(\tau = 0) = 0.18$. Both these values of $g^{(2)}(\tau = 0)$ are already significantly below the 0.5 limit, proving that a QDash prepared in the charge or neutral exciton state can be considered as a single photon emitter. The non-zero value of $g^{(2)}(\tau = 0)$ for both the investigated species is probably due the combination of the system background counts, large time bin (512 ps) and limited time resolution of the HBT setup (approximately 100 ps). In order to take those into account and correct the $g^{(2)}(\tau = 0)$ accordingly, the histograms have been expressed by a standard $g^{(2)}_R(t) = 1 - (1 - g^{(2)}_R(\tau = 0)) \exp\left(-\frac{|t|}{\tau_f}\right)$ fitting function, plus a deconvolution with the system instrumental response function (IRF) in the form of $\exp\left(-\frac{|t|}{\tau_{IRF}}\right)$, where τ_{IRF} is the setup time resolution (100 ps). The resulting $g^{(2)}_R(\tau = 0)$ for both histograms reaches almost zero value, see dotted lines in Fig. 3.

In conclusion, we have performed microphotoluminescence and photon correlation experiments on a single self-assembled InAs/InGaAlAs/InP QDash emitting at 1.55 μm. Polarization-resolved PL combined with photon cross-

FIG. 3. Photon auto-correlation function for (a) charged exciton and (b) neutral exciton measured at low temperature. Blue dotted lines correspond to standard mono-exponential $g^{(2)}_R(t)$ function after the dark-count subtraction and deconvolution with the system instrumental response function.

correlation measurements allowed us to identify spectral features attributed to a neutral and charged exciton emission originating from the same dash. Ultimately, we have shown that the emission process from neutral and charged exciton exhibits a clear photon antibunching in the photon number statistics with the as-measured values of the second order correlation function at the zero time delay significantly below 0.5. Those observations prove that the investigated InAs/InGaAlAs/InP QDash prepared in the neutral or charged exciton state can be considered as a true single photon emitter. Moreover, this kind of a quantum emitter can potentially be easily integrated with other components of the existing fiber-based communication technology, which is its additional advantage when compared to other proposed solutions.
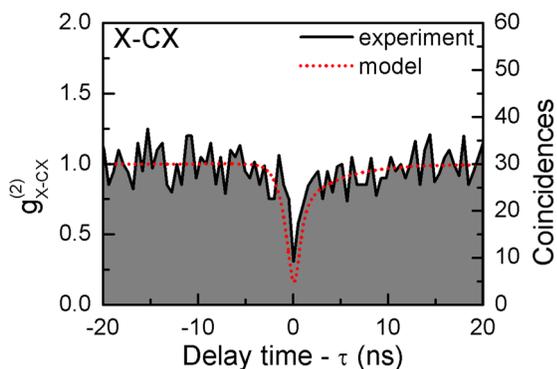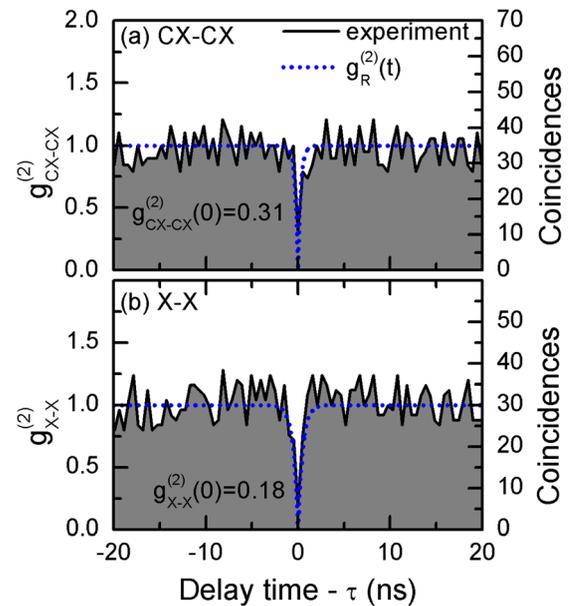
FIG. 2. Second order exciton-charged exciton (X-CX) emission cross-correlation function. The fit is performed (red solid line) using five level rate equation model.

[1]D. Elvira, R. Hostein, B. Fain, L. Monniello, A. Michon, G. Beaudoin, R. Braive, I. Robert-Philip, I. Abram, I. Sagnes, and A. Beveratos, Phys. Rev. B **84**, 195302 (2011).
[2]K. Takemoto, M. Takatsu, S. Hirose, N. Yokoyama, Y. Sakuma, T. Usuki, T. Miyazawa, and Y. Arakawa, J. Appl. Phys. **101**, 081720 (2007).

³M. Benyoucef, M. Yacob, J. P. Reithmaier, J. Kettler, and P. Michler, Appl. Phys. Lett. **103**, 162101 (2013).

⁴M. D. Birowosuto, H. Sumikura, S. Matsuo, H. Taniyama, P. J. van Veldhoven, R. Nötzel, and M. Notomi, Sci. Rep. **2**, 321 (2012).

⁵N. Gisin, G. Ribordy, W. Tittel, and H. Zbinden, Rev. Mod. Phys. **74**, 145 (2002).

⁶J. P. Reithmaier, G. Sęk, A. Löffler, C. Hofmann, S. Kuhn, S. Reitzenstein, L. Keldysh, V. Kulakovskii, T. Reinecke, and A. Forchel, Nature **432**, 197 (2004).

⁷B. Lounis and M. Orrit, Rep. Prog. Phys. **68**, 1129 (2005).

⁸Z. Yuan, B. E. Kardynal, R. M. Stevenson, A. J. Shields, C. J. Lobo, K. Cooper, N. S. Beattie, D. A. Ritchie, and M. Pepper, Science **295**, 102 (2002).

⁹S. Strauf, N. G. Stoltz, M. T. Rakher, L. A. Coldren, P. M. Petroff, and D. Bouwmeester, Nat. Photonics **1**, 704 (2007).

¹⁰J. Claudon, J. Bleuse, N. S. Malik, M. Bazin, P. Jaffrennou, N. Gregersen, C. Sauvan, P. Lalanne, and J.-M. Gérard, Nat. Photonics **4**, 174 (2010).

¹¹C. Santori, D. Fattal, J. Vucković, G. S. Solomon, and Y. Yamamoto, Nature **419**, 594 (2002).

¹²E. Flagg, A. Muller, and J. Robertson, Nat. Phys. **5**, 203 (2009).

¹³Y.-M. He, Y. He, Y.-J. Wei, D. Wu, M. Atatüre, C. Schneider, S. Höfling, M. Kamp, C.-Y. Lu, and J.-W. Pan, Nat. Nanotechnol. **8**, 213 (2013).

¹⁴R. Bose, X. Yang, R. Chatterjee, J. Gao, and C. W. Wong, Appl. Phys. Lett. **90**, 111117 (2007).

¹⁵A. Winden, M. Mikulics, D. Grützmacher, and H. Hardtdegen, Nanotechnology **24**, 405302 (2013).

¹⁶E. S. Semenova, R. Hostein, G. Patriarche, O. Mauguin, L. Largeau, I. Robert-Philip, A. Beveratos, and A. Lemaître, J. Appl. Phys. **103**, 103533 (2008).

¹⁷J. S. Pelc, L. Yu, K. De Greve, P. L. McMahon, C. M. Natarajan, V. Esfandyarpour, S. Maier, C. Schneider, M. Kamp, S. Höfling, R. H.

Hadfield, A. Forchel, Y. Yamamoto, and M. M. Fejer, Opt. Express **20**, 27510 (2012).

¹⁸A. Dousse, J. Suffczyński, A. Beveratos, O. Krebs, A. Lemaître, I. Sagnes, J. Bloch, P. Voisin, and P. Senellart, Nature **466**, 217 (2010).

¹⁹L. Seravalli, G. Trevisi, P. Frigeri, D. Rivas, G. Muñoz-Matutano, I. Suárez, B. Alén, J. Canet, and J. P. Martínez-Pastor, Appl. Phys. Lett. **98**, 173112 (2011).

²⁰D. Press, K. De Greve, P. L. McMahon, T. D. Ladd, B. Friess, C. Schneider, M. Kamp, S. Höfling, A. Forchel, and Y. Yamamoto, Nat. Photonics **4**, 367 (2010).

²¹A. Sauerwald, T. Kuümmell, G. Bacher, A. Somers, R. Schwertberger, J. P. Reithmaier, and A. Forchel, Appl. Phys. Lett. **86**, 253112 (2005).

²²R. Hanbury Brown and R. Q. Twiss, Nature (London) **177**, 27 (1956).

²³L. Sapienza, R. N. E. Malein, C. E. Kuklewicz, P. E. Kremer, K. Srinivasan, A. Griffiths, E. Clarke, M. Gong, R. J. Warburton, and B. D. Gerardot, Phys. Rev. B **88**, 155330 (2013).

²⁴H. Nakajima, H. Kumano, H. Iijima, S. Odashima, and I. Suemune, Phys. Rev. B **88**, 045324 (2013).

²⁵J. Suffczyński, T. Kazimierczuk, M. Goryca, B. Piechal, A. Trajnerowicz, K. Kowalik, P. Kossacki, A. Golnik, K. Korona, M. Nawrocki, J. Gaj, and G. Karczewski, Phys. Rev. B **74**, 085319 (2006).

²⁶Ł. Dusanowski, M. Syperek, W. Rudno-Rudziński, P. Mrowiński, G. Sęk, J. Misiewicz, A. Somers, J. P. Reithmaier, S. Höfling, and A. Forchel, Appl. Phys. Lett. **103**, 253113 (2013).

²⁷J. Smith, P. Dalgarno, R. Warburton, A. Govorov, K. Karrai, B. Gerardot, and P. Petroff, Phys. Rev. Lett. **94**, 197402 (2005).

²⁸O. B. Shchekin and D. G. Deppe, Appl. Phys. Lett. **80**, 3277 (2002).

²⁹G. Sallen, A. Tribu, T. Aichele, R. André, L. Besombes, C. Bougerol, S. Tatarenko, K. Kheng, and J. P. Poizat, Phys. Rev. B **80**, 085310 (2009).

³⁰M. Zieliński, J. Phys.: Condens. Matter **25**, 465301 (2013).